*Journal of* ELECTRICAL ENGINEERING, VOL. 58, NO. 4, 2007, 181–188

# IMPROVED APPROACH FOR MOBILE ROBOTICS IN PATTERN RECOGNITION 3D

**Abdelhalim Boutarfa** [*] — **Nour-Eddine Bouguechal** [*] — **Hubert Emptoz** [**]

In this paper, a new approach of mobile robotics in pattern recognition is introduced. Its originality lies in the fact that it is based on a hybrid parametric technique which uses the neural network and the Generalized Incremental Hough Transform (GIHT) for recognition of objects. The problem is first formulated as an optimization task where a cost function, representing the constraints on the solution, is to be minimized. The optimization problem is then performed by Hopfield neural network. We solve the correspondence problem for a set of segments extracted from a pair of stereo images. The segments are extracted from binary image edges using the Hough transform (HT). Its advantage is its ability to detect discontinuous patterns in noisy images but it requires a large amount of computing power. For field programmable gate arrays (FPGA) implementation our algorithm does not require any Look up Table or trigonometric calculations at run time. This algorithm leads to a significant reduction of the HT computation time and can be therefore used in real-time applications.

K e y w o r d s: robotic vision system, Hopfield network, Hough transform, segments matching, signal processing, pattern recognition

## 1 INTRODUCTION

Stereo vision is a passive technique used to determine the depth of an object in a scene using a pair of stereo images [1]. The depth information is essential in many applications such as robotics, remote sensing, and medical imaging. The stereo correspondence is a very important step in the depth calculation.

There are two different methods for solving the correspondence problem: one is to match every point in the left image with that of the right image [2, 3]; another is to match directly the features of an image with features of another image of the same scene from a different viewing position.

In this paper, we are interested in solving the correspondence problem using the neural network. The developed approach realizes segments matching of a pair of stereo images. A cost function is used where all the constraints on the solution can explicitly be included in this function. We search the minimum of this function with a two-dimensional Hopfield neural network to find the solution of the correspondence problem. Many vision tasks can be formulated as minimization of a cost function [4, 5].

For example, in [6] an image restoration technique is developed, where a cost function is minimized by a Hopfield network.

For feature extraction, we have chosen the technique developed by Hough [7]. It is a well-known technique for detection of parametric curves in binary images and it was recognized as an important means of searching for objects and features in binary images. It converts the problem of detecting collinear points, or lines, in the feature space to the problem of locating concurrent or intersecting curves in the parameter space. We have used the neighbourhood relationship between segments to represent each image of a pair of stereo images by an adjacency graph to eliminate the possibility of choosing segments that have no chance of being a candidate for a match.

In that sense, our paper is organized as follow: in Section 2, we show the feature extraction algorithm based on the HT. In Section 3, the Hopfield model to solve the correspondence problem is presented and justified. Next, the software implementation is in Section 4. The obtained results on real images with a robot motion can be appreciated in Section 5. Finally, we bring this paper to a conclusion and present the perspectives of this research.

## 2 HOUGH TRANSFORM

The first step of the correspondence algorithm is to find line segments in both images. These segments are extracted from binary edges images using the Hough transform. It is a well-know method for detection of parametric curves in binary images and it was recognized as an important means of searching for objects and features in binary images. It converts the problem of detecting collinear

[*] Advanced Electronics Laboratory (LEA), University of Batna, Rue Chahid Boukhlouf, CUBI, Batna, 05000, Algeria.
E-mails: boutarfahal@yahoo.fr, bougnour@yahoo.fr

[**] INSA Laboratoire de Reconnaissance des Formes (RFV-LIRIS), 20 avenue Albert Einstein, 69621 Villeurbanne Cedex, France.
E-mail: emptoz@rfv.insa-lyon.fr

ISSN 1335-3632 

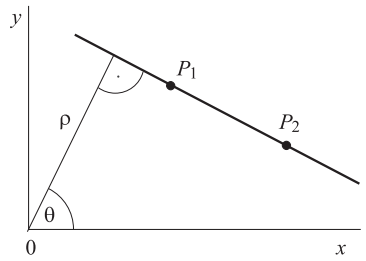


**Fig. 1.** The straight line polar parameter

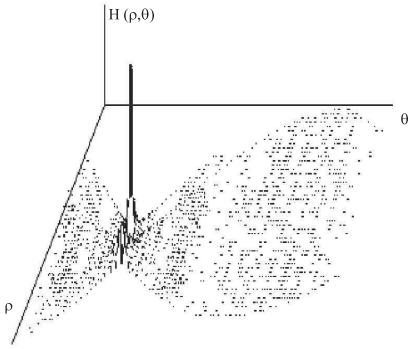


**Fig. 2.** The $\rho\theta$ parameter space

points, or lines, in the feature space to the problem of locating concurrent, or intersecting, curves in parameter space.

The HT uses the polar parameters of the straight line (Fig. 5). A line is defined by the following equation:

$$f(x, y, \rho, \theta) = \rho - x\cos\theta - y\sin\theta = 0\,. \qquad (1)$$

Here "$\rho$" is the normal distance between the $xy$ plane origin and the line $y(x)$ and where "$\theta$" is the angle between $x$ axis and "$\rho$".

Point $(x_i, y_i)$ of the $xy$ plane is transformed in the new plane of parameters $\rho\theta$ into a sinusoidal curve whose equation is given by:

$$\rho = x_i\cos\theta + y_i\sin\theta\,. \qquad (2)$$

Let us have two points of a same line (Fig. 1), their transforms into the parameter plane are represented by two sinusoidal curves which intersect in one point which will characterize this line in the $xy$ plane. Generalize; the set of points forming this line will be represented by a set of sinusoidal curves that intersect in one point which also characterize this line into the $xy$ plane (Fig. 2).

The $\rho\theta$ plane is homogenous because all the curves are sinusoidal curves and, furthermore, this kind of parameterization yields a bounded "$\rho$" and "$\theta$" in the practical case of a numerical image.

Let $\theta_k$ be the quantification step of $\theta$ dimension and $\rho_k$ the quantification step of $\rho$ dimension, we compute for every discrete value of $\theta_i$ its corresponding $\rho_i$ for every point of coordinates $(x, y)$ in the image, following the equation:

$$\rho_j = x\cos\theta_i + y\sin\theta_i\,. \qquad (3)$$

Then, we increase by value 1, the whole cell $(p_i, \theta_i)$ of the accumulator table. This cell will be increased every time an edge point lies on the straight line whose polar parameters are $\rho_j$ and $\theta_i$. Initially, all the cells values of the accumulator table are set to zero.

The choice of the $\rho\theta$ parameters space quantification must carry the three essential goals that are:

- good detection precision,
- less memory storage of accumulators,
- fast implementation.

The value of $M$ of any cell $(\rho_m, \theta_1)$ in the accumulator table indicates that $M$ edge points of the image are lying along the straight line whose polar parameters are $\rho_m$ and $\theta_1$.

We introduce a threshold of the accumulated value in a cell and some probabilities for the presence of points along this straight line. Finally, the line segments extraction from the binary edge image is performed by searching line segments carried by every significant straight line $(\rho_i, \theta_i)$ in the accumulator table.

A significant straight line in the binary edge image is characterized by a peak in the accumulator table, and for every detected peak we eliminate the effect on the number of the points belonging to this peak in the accumulator table [8].

The line segment extraction result is a segments list where each segment is stored with the following attributes:

- An index: its position among the whole segments.
- $\rho$: its normal distance relative to the image coordinate system.
- $\theta$: its orientation in this coordinate system.
- $(x_1, y_1)$ and $(x_2, y_2)$: its extremities coordinates.

We added the neighbourhood relationship between segments to the precedent local attributes. They allow building links between all segments. Indeed, as a matter of fact, a set of neighbouring segments may belong to the same object in the scene. To retrieve the neighbourhood of a line segment, we have applied the method shown in [9, 10]. It consists in partitioning the image into a set of windows of square shape and of fixed size ($1_x$ and $1_y$).

Two line segments are said to be neighbours if they have at least one window in common. To the local attributes, defined previously, a list: voi[lv] of "lv" of the neighbors segments is added.

So, we have created a data structure which contains all line segments of an image with their local properties and also the neighbourhood. Then, the image is represented by an adjacency graph which nodes are line segments attached to geometrical properties and which arc defines neighbourhood relationship between segments [11, 12].

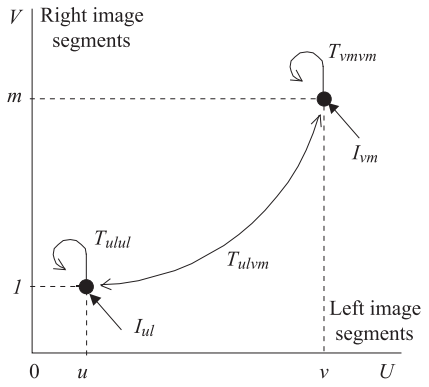


**Fig. 3.** The 2D Hopfield network with its neurons interconnections

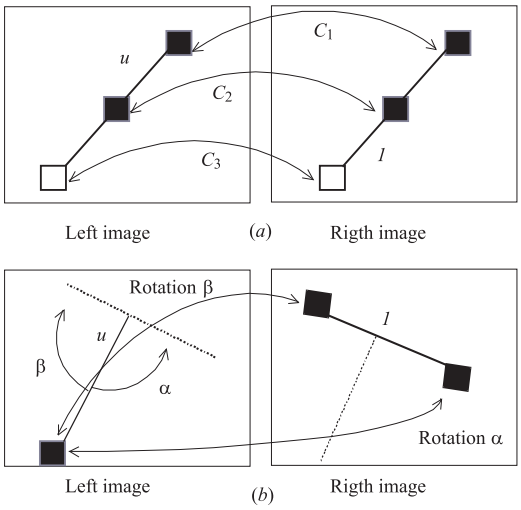


**Fig. 4.** The correlation measure algorithm between two matched segments: (a)– the first correlation algorithm, (b) – the second correlation algorithm

## 3 USING HOPFIELD MODEL AND SOLVING SEGMENTS MATCHING PROBLEM

In this section, it is shown that the stereo correspondence problem can be formulated as an optimization task where a cost function representing the constraints on the stereo solution is minimized [4, 13]. The optimization problem can be mapped onto two-dimensional binary Hopfield network [14, 15].

This network is used to find the correspondence between a segment in the left image and another one in the right image. It is represented as an $U \times V$ array of neurons where $U$ and $V$ are the total number of segments in the left and the right image respectively.

The state (on or off) of each neuron in the network represents a possible match between segments in the left image with one in the right image. Fig. 3 shows the 2D network and the connection weights between its neurons.

The Lyapunov function for a two-dimensional binary Hopfield network [6] is given by:

$$E = -\frac{1}{2}\sum_{u,l}\sum_{v,m} T_{ulvm} V_{ul} V_{vm} - \sum_{u,l} I_{ul} V_{ul}, \qquad (4)$$

where $V_{ul}$ and $V_{vm}$ represent the binary states (output) of $(u,l)$ and $(v,m)$ neurons, respectively, which can be either 1 (active) or 0 (inactive), $T_{ulvm}$ $(-TT_{vmul})$ is the interconnection strength between the two neurons, the self-feedback to each neuron is $T_{ulul} = 0$, and $I_{ul}$ is the initial input to each neuron.

In this network we can use the following constraints:

Global constraints — these link the hypotheses by pair in order to check the compatibility of these hypotheses. For our problem, we only have one global constraint namely the uniqueness by line and column. Indeed, we want each line and each column of the matrix to have only one activated neuron.

Compatibility constraint — is based on the compatibility measure of match between a pair of segments $(u,v)$ in the left image and a pair of segments $(l,m)$ in the right image. The compatibility measure is given by the following equations:

$$C_{ulvm} = \frac{2}{1 - e^{\lambda(X-\theta)}} - 1 \qquad (5)$$

$$X = \Delta cor + \Delta long + \Delta Teta. \qquad (6)$$

Equation (6) shows that the compatibility is based on tree of comparisons for two matched segment pairs. The first comparison $\Delta cor$ is the difference in the correlation between a pair of segments $(u,v)$ in the left image and a pair of segments $(l,m)$ in the right image. We have applied two algorithms of correlation measure used by [16]. The first is used when the movement between the two segments images is small. We compute a coefficient of correlation between the grey level signal in several small windows equi-distributed along the two matched segments (Fig. 4a). The second algorithm takes into account more important movements between the images of the sequence. In this case, we have to apply to the windows, the same rotation that exists between the segments in the two images (Fig. 4b).

In the two above methods, the correlation coefficient between the windows is given by the equation:

$$C = \frac{\sum_{x,y} I_{xy}^{(1)} I_{xy}^{(2)}}{\sqrt{\sum_{x,y}\left(I_{xy}^{(1)}\right)^2 \sum_{x,y}\left(I_{xy}^{(2)}\right)^2}}. \qquad (7)$$

$I_{xy}^{(i)}$ is the grey level of the pixel $(x,y)$ in image $i$.

The correlation is defined between two segments by the mean value of the correlations between the different windows along the segments. The parameters involved in the computation of the constraint value are the width and height of the windows and the number of windows along the segments. They have been chosen as lines and were never modified during all the experiments on the different stereo pair of images.

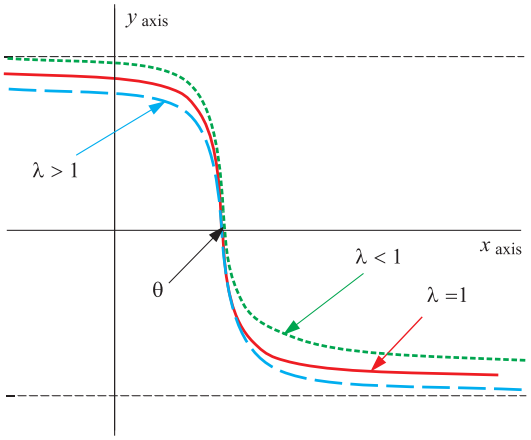


**Fig. 5.** Graph of the nonlinear function used to obtain the compatibility

The second and the third comparison of the equation (6) are the difference in the length and orientation between a pair of segments $(u, v)$ in the left image and a pair of segments $(l, m)$ in the right image.

The nonlinear function used in (5) scales the compatibility measure smoothly between $+1$ and $-1$. Figure 3 shows this nonlinear function for several values of $\lambda$. Where $\lambda$ is a parameter that sets the slope of the function? A very large value of $\lambda$ will result in a step function for the compatibility measure with possible values of $+1$ or $-1$. If a very small value of $\lambda$ is used, the function will smoothly switch from $+1$ to $-1$, with possible compatibility values between. The parameter $\theta$ controls the position where the nonlinear function crosses the $X$ axis. This parameter is chosen such that a compatibility of $+1$ is obtained for a good match $(X = 0)$: a mutual compatibility of 0 for a match when the $X$ value is not exactly zero, allowing an acceptable tolerance for noise and distortion; and a compatibility of $-1$ for a bad match $(X \gg 0)$.

Neighbourhood constraint: If a segment $u$ is matched with a segment $l$ then it is impossible for a segment v neighbour of the segment u do not matched with a segment m neighbour of the segment $l$.

The neighbourhood measure is given by the following equation:

$$N_{ulvm} = |W_{uv} - W_{lm}|$$
$$\text{with } W_{ij} = \begin{cases} 1 & \text{if } j \text{ is neighbor of } i \\ 0 & \text{otherwise} \end{cases} \quad (8)$$

Distance constraint: The calculated distance represents the distance between the middle of the two segments in the both images.

To solve the stereo correspondence problem, the cost function given below is minimized:

$$H = A\sum_u \Big(1 - \sum_l P_{ul}\Big)^2 + B\sum_l \Big(1 - \sum_u P_{ul}\Big)^2 - C\sum_{ul}\sum_{v,m} C_{ulvm}P_{ul}P_{vm} + D\sum_{ul}\sum_{v,m} N_{ulvm}P_{ul}P_{vm} + E\sum_{u,l} Dist(u,l)P_{ul} \quad (9)$$

The first and second terms in the equation (9) represent the uniqueness constraint, the third and the fourth term represent the degree of compatibility and the neighbourhood constraint of a matching between a pair of segments $(u, v)$ in the left image and a pair of segments $(l, m)$ in the right image, and the last term represents the distance constraint for the matching between a segment $u$ in the left image and a segment $l$ in the right image. $P_{ij}$ represents a measure of match between a segment $i$ in the left image and a segment $j$ in the right image. $A, B, C, D$ and $E$ are coefficients to weight the different constraints of the cost function.

Equation (6) can be rearranged to get [17, 18]:

$$E = -\frac{1}{2}\sum_{u,l}\sum_{v,m}\big[CC_{ulvm}(1-\delta_{uv})(1-\delta_{lm}) - DN_{ulvm}(1-\delta_{uv})(1-\delta_{lm}) - A\delta_{uv}(1-\delta_{lm}) - B\delta_{lm}(1-\delta_{uv})\big]P_{ul}P_{vm} - \sum_{u,l}\big[A + B - \frac{E}{2}Dist(u,l)\big]P_{ul}\,. \quad (10)$$

Here $\delta_{xy}$ is the Kronecker symbol.

This cost function can be shown to be equivalent to the Lyapunov function of a Hopfield network (equation 4) with states of the neurons defined as $V_{ul} = P_{ul}$ and $V_{vm} = P_{vm}$, and the input to each neuron set to:

$$I_{ul} = A + B - \frac{E}{2}Dist(u,l)\,. \quad (11)$$

The connection weight between the neurons $(u, l)$ and $(v, m)$ is defined as:

$$T_{ulvm} = CC_{ulvm}(1-\delta_{uv})(1-\delta_{lm}) - DN_{ulvm}(1-\delta_{uv})(1-\delta_{lm}) - A\delta_{uv}(1-\delta_{lm}) - B\delta_{lm}(1-\delta_{uv})\,. \quad (12)$$

The total input to the neuron (u,l), is given by:

$$u_{ul} = \sum_v\sum_m T_{ulvm}V_{vm} + I_{ul}\,. \quad (13)$$

At any time, the binary state $V_{ul}$ of the neuron $(u, l)$ is:

$$V_{ul} = g(u_{ul}) \quad (14)$$

in which $g(x)$ is the activation function, it is given by:

$$V_{ul} = \begin{cases} 0 & \text{if } u_{ul} < 0\,, \\ 1 & \text{if } u_{ul} > 0\,, \\ nochange & \text{if } u_{ul} = 0\,. \end{cases} \quad (15)$$

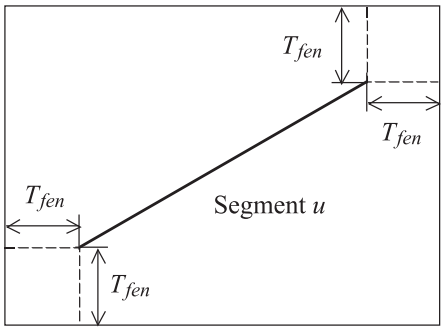


**Fig. 6.** The shape of the $F(u)$ research window

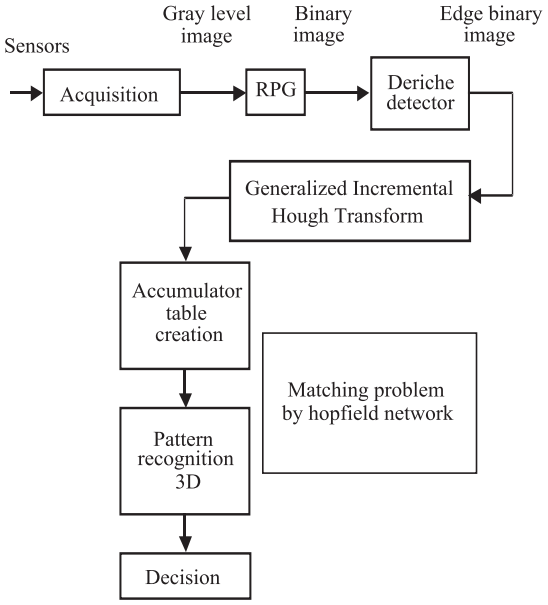


**Fig. 7.** Process of pattern recognition

In the equation 13, the neighbouring of each segment $u$, are taken as the $v$'s for that comparison; all the other segments are assumed to have zero compatibility and neighbour constraint contributions respectively, because they are to far and probably belong to another object in the scene. Each segment l is also chosen in a research window $F(u)$ opened around the segment $u$ in the right image, it is considered a possible match by assigning an initial output $V_{ul} = 1$ to each of them.

The research window dimensions depend upon the size of the current segment u and the value of the threshold $T_{fen}$. This window is used to eliminate the possibility of choosing segments that have no chance of being a candidate for matching. Figure 4 show the shape of the $F(u)$ research window.

The updating procedure (equation 15) is iterated until the network converges to a stable state. The network is said to be at its stable state (local or global minima of the energy function) when there is no change in the states of neurons. The network is then stopped after several iterations.

## 4 SOFTWARE IMPLEMENTATION

The Standard Hough Transform (SHT) and the improved GIHT have similar basic steps in their line segments extraction algorithm. The line segment extraction algorithm from the Hough space is performed by searching segments carried by each significant line segment in this space. A significant line segment is characterized by a peak in the Hough space, and for each detected peak, we remove from the Hough space the effect of its points [8]. This algorithm is applied on binary edge images obtained in our case by using the Deriche edge detection algorithm described in [19].

The used segment extraction algorithm outputs the polar coordinate $(\theta, \rho)$ of a line and the coordinates of its end points, it uses the two procedures which summarize the voting process and the segment extraction algorithms.

Procedure 1: The voting process Algorithm

*Begin*
*For each binary edge image point Do,*
*For each sub interval* $[mK/M, (m+1)K/M[$
*of the* $\theta$*-axis*
*Do*
*Calculation of the* $\rho$*'s initial values* $\rho_{(mK/M)}$
*and* $\rho_{mK/M)+(K/2)}$
*For* $0 < n < (K/M - 1)$ *Do,*
*Calculation of the* $\rho_{(n+1)+(mK/M)}$ *and the*
$\rho_{(n+1)+(mK/M)+(K/2)}$ *values*
*For each calculated* $\rho i$ *we increasing by one*
*the cell* $(i\varepsilon\rho i$ *from the Hough space*
*EndDo.*
*EndDo.*
*EndDo.*
*End.*

Procedure 2: The line segment extraction Algorithm

*Begin*
*The Max peak* $(n_{Max}\varepsilon, \rho_{Max})$ *value extraction*
*from the Hough space.*
*While this value is superior of an experimentally*
*threshold ThH Do*
*For each binary edge image point forming this peak Do*
*For* $0 < n < (K/M - 1)$ *in each sub interval*
$[mK/M, (m+1)K/M[$ *of the* $\theta$*-axis Do*
*Decreasing by one the cell* $(n\varepsilon, \rho_n)$
*from the Hough space*
*EndDo.*
*EndDo.*
*For the whole binary edge image points*
*forming this peak Do*
*looking for all adjacent points whose lengths are*
*superior to the same threshold ThH.*
*End Do.*
*End While.*
*End.*

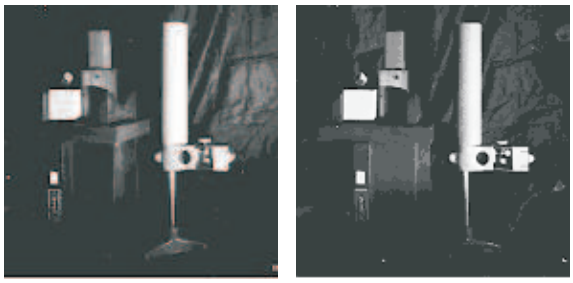

**Fig. 8.** The stereo pair 3D laboratory

## 5 EXPERIMENTAL RESULTS

The experimented results have been tested by the robot available in the laboratory of artificial vision of advanced centre of technology in Algiers (Fig. 7).

The algorithm to solve the correspondence problem has been implemented in Borland C++ Builder language under Windows.

It was tested on several pair stereo images. It is necessary that each scan line in the left image corresponds appreciatively to the same scan line in the right image. Therefore, each segment in the left image is almost on the same scan line in the right image but shifted to the right. The binary edge is detected by using the Canny-Deriche operator. The choice of the five coefficients of the equation (6) isn't simple and there isn't any known method to find them efficiently in an automated way. We have chosen them experimentally.

In Table 1, we have illustrated the experimental results of our method applied on pair of stereo images (Figures 8 to 11) with several values of five coefficients in (9). It shows that if we only use one of the constraint (global, neighbourhood, compatibility or distance), we generally have the best segment matching number that is less than the bad segment matching number. The distance constraint gives lower results if it is used only.

When we use all constraints, the results are better than with only one constraint but the number of the segment matching is small. Because, if one measure (distance, neighbourhood, compatibility or global constraints) gives lower results, the network can give a good final best segment matching if the other measure is accurate enough.

Therefore, we must choose the five coefficient values $A, B, C, DandE$ that give best results with the minimum of bad segment matching.

The presented results of matching have performed with the following parameters that have been chosen experimentally:

$$T_{fen} = 30,\ \lambda = 1,\ \theta = 0,\ \rho_k = 1,$$
$$\theta_k = 1^\circ,\ 1_x = 1_y = 256.$$

The original input images are presented in Figures 9a to 11a. The recognition results using generalized Hough transform are presented in Figures 9c to 11c.

**Table 1.** Experimental results

| Images | 3DLAB_L | 3DLAB_R | Objects |
|---|---|---|---|
| Size | $256 \times 256$ | $256 \times 256$ | $256 \times 256$ |
| ThH | 3 | 3 | 3 |
| Figures | 9c | 10c | 11c |
| $N_{\text{seg}}$ | 217 | 209 | 259 |
| $N_{\text{peak}}$ | 96 | 104 | 118 |

$N_{\text{peak}}$, $N_{\text{seg}}$, and ThH are,respectively, the number of detected peaks from the Hough space, the number of detected line segments and the threshold length value for line segments detection.

## 6 CONCLUSION

In this paper, we have presented a new pattern recognition method based application in image processing. Our contribution is extracting objects present in an image of a scene and to distinguish them from the background by a neural network classifier. Its originality lies in the fact that it is based on a hybrid parametric technique which uses the neural network and the generalized Hough transform for the recognition of objects.

The results obtained by our algorithm are very satisfying since the objects are clearly extracted and detected from the original images. Also, the obtained results including the neural networks from this study give us a valuable insight into the role of network topology, rate parameters, training sample set and initial weights.

We have also presented a new method to solve the correspondence problem for a set of segments extracted from a pair of stereo images. This problem is formulated as a minimization of a cost function which is then mapped onto a two-dimensional binary Hopfield neural network. This function is at its minimum when the system is at its stable state. In this case, the constraints on the solution of the stereo correspondence problem are satisfied. We have used five coefficients to weight the different constraints of the cost function, in order to lead the network to the global minimum of its energy function.

While joining HT (technical multi-resolution, decision, fusion), our system remains robust at the price of an extremely appreciable computing time. The time requirements to process a frame, after the learning stage, with an IBM-PC having a Pentium processor is about a few milliseconds during the operation of the mobile robot, which seems better than other published results obtained in the same conditions of work [20–24].

Our experiments have been carried out on the mobile robot (Automated Guided Vehicle AGV), shown in figure 8, which is equipped with two camera CCD. We worked out a strategy of assistance to navigation in an environment of workshop.

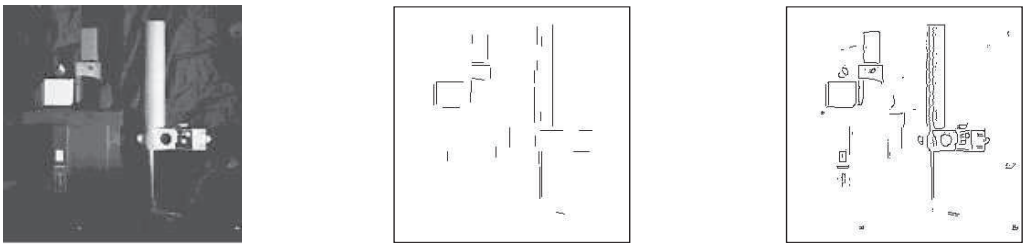

(a) (b) (c)

**Fig. 9.** Algorithms results — method applied on the 3DLab_Left image (a) Gray-level image; (b) binary edge image; (c) recognition results

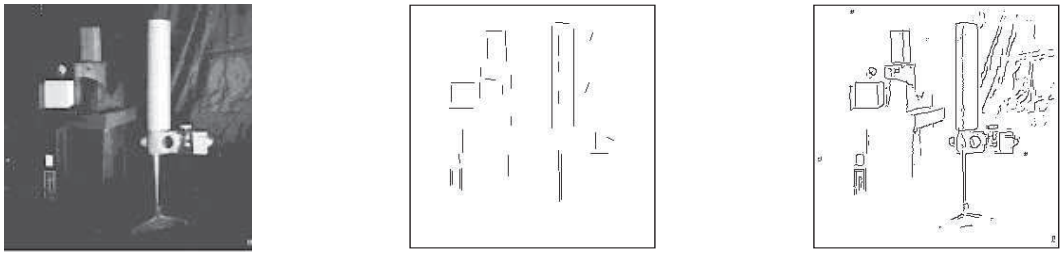

(a) (b) (c)

**Fig. 10.** Algorithms results — method applied on the 3DLab_Right image (a) Gray-level image; (b) binary edge image; (c) recognition results

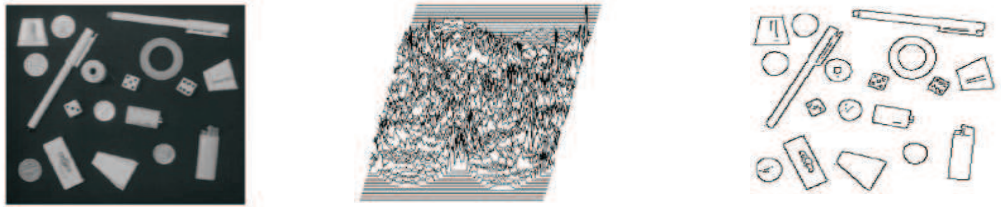

(a) (b) (c)

**Fig. 11.** Algorithms results applied on the objects image (a) Gray-level image; (b) Hough space (c) recognition results

To increase the robustness of the system, two semi-local constraints on combinations of neighbourhood correspondences are derived (one geometric, the other photometric). They allow testing the consistency of correspondences and hence to reject falsely matched neighbourhoods. Experiments on images of real-world scenes taken from substantially different viewpoints demonstrate the feasibility of the approach [27, 28].

The efficiency of the method was attested by the good results we have obtained. Some improvements can be brought to our method like the automatic setting of the five coefficients of the equation (5), and a better segment detection will certainly enhance the quality of the matching results.

The FPGA device will be included in the visual navigation system of our laboratory mobile robot. After edge restoration, the device results will be used either as the basic data to determine the depth of an object in three dimensions by geometric reasoning, or as input data to other algorithms such as the matching algorithm developed in [22] and [25] and the navigation algorithms developed in [23] and [26] to endow the mobile robot with the intelligence required to perceive its environment.

Our work enabled us to bring a solution to the problems of the pattern recognition in mobile robotics.

In perspectives, this work will lead us to a better understanding of the problems related to robotics in dynamic vision.

## Acknowledgments

The authors would like to thank all vision team members of the Robotic Laboratory and Artificial Intelligence for their useful comments and suggestions.

## References

[1] DHOND, U.—AGGARWAL, J. K.: Structure from Stereo - A Review, IEEE Trans. Syst. Man. Cybern. **19** (November 1989), 1489–1510.

[2] MARR, D.—POGGIO, T.: Cooperative Computation of Stereo Disparity, Science.

[3] PRAZDNY, K.: Detection of Binocular Disparity, Biol. Cybern. **52** (1985), 93–97.

[4] BERTERO, M.—POGGIO, T. A.—TORRE, V.: BI-Posed Problems in Early Vision, Proc. IEEE **76** (August 1988), 869–889.

[5] ZHOU, Y. T.—CHELLAPA, R.: Neural Network Algorithms for Motion Stereo, Proc. IEEE Int. Joint. Conference on Neural Networks **2** (June 1989), 251–258.

[6] ZHOU, Y. T.—CHELLAPA, R.—VAID, A.—JENKIUS, B. K.: Image Restoration Using a Neural Network, IEEE Trans. Acoust., Speech, Signal Proces. **36** No. 7 (July 1988).

[7] RICHARD, O.—HART, P. E.: Communication of the A.C.M..

[8] DJEKOUNE, O.—BENKHELIF, M.—ZENATI, N.: Application de la Transformée de Hough dans l'appariement des images de scènes, CARI'2000. 5$^{éme}$ Colloque Africain sur la Recherche en Informatique, Madagascar, (Octobre 16-19. 2000), 343–350.

[9] AYACHE, N.—FAUGERAS, O. D.—FAVERJON, B.—TOSCANI, G.: Mise en correspondance de cartes de profondeur obtenues par stéréoscopie passive, AFCET, (1985).

[10] AYACHE, N.—FAUGERAS, O. D.: A New Method for the Recognition andPositioning of 2-D Objects, 7$^{th}$ ICPR, Montreal, Canada, (July 1984), 1274–1277.

[11] PALETTA, L.—ROME, E.—PINZ, A.: Visual Object Detection for Autonomous Sewer Robots, IROS'99, Proceeding of the 1999 IEEE/RSJ. International Conference on Intelligent Robots and Systems, Kyougju, South Korea, (October, 17–21, 1999), 1087–1093.

[12] EBRAHIMI, C. T.: Video Objects Extraction Based on Adaptative Background and Statistical Change Detection, In SPIE Electronics Imaging, San Jose, California, USA, (January, 2001).

[13] NASRABADI, N. M.—LI, W.: Object Recognition by a Hopfield Neural Network, IEEE Trans. Syst. Man, Cyber **21** (1991).

[14] HOPFIELD, J. Neural Networks and Physical Systems with Emergent Collective Computational Abilities: Proc. Nat. Acad. Science **79** ((April, 1982)), 2554–2558.

[15] HOPFIELD, J.—TANK, D. W.: Neural Computation of Decisions in Optimization Problems, Biology Cybernetic **52** (1985), 141–152.

[16] LAUMY, M.—DHOME, M.—LAPRESTÉ, J-T.: Segments Matching: Comparison between a Neural Approach and a Classical Optimization Way, IEEE, Proceedings of ICPR' 96, (1996), 261–265.

[17] NASRABADI, N. M.—CHOO, C. Y.: Hopfield Network for Stereo Vision Correspondence, IEEE Trans. On Neural Networks **3** No. 1 (January 1992), 5–12.

[18] RUICHEK, Y.—POSTAIRE, J-G.—MACAIRE, L.—BURIE, J.-C.: Implantation neuronale pour la mise en correspondance de primitives en stéréovision linéaire, Proc. Intern. AMSE Confer. Communications, Signals & Systems, Rabat, Maroc **2** (Octobre 9-11, 1995), 574–582.

[19] DERICHE, R.: Using Canny's Criteria to Derive a Recursively Implemented Optimal Edge Detector, International Journal of Computer Vision **1** No. 2 (1987), 167–187.

[20] QING SONG—JIZHONG XIAO—YENG CHAI SOH: Robust Back Propagation Training Algorithm for Multilayered Neural Tracking Controller, IEEE Transactions on Robotics and Automation **10** No. 5 (September 1999).

[21] BALUJA, S.: Evolution of an Artificial Neural Network Based Autonomous Land Vehicle Controller, ALVINN, IEEE Transactions on Systems, Man and Cybernetics, Part B **26** No. 3 (June 1996), 450–463.

[22] DJEKOUNE, A. O.—ACHOUR, K.—ZOUBIRI, H.: Segments Matching Using a Neural Network Approach, ACS/IEEE International conference on computer systems and applications, AICCSA' 01, Beirut, Lebanon **16** No. 1 (June 25-29, 2001), 103–105.

[23] ACHOUR, K.—DJEKOUNE, O.: Localisation and Guidance with an Embarked Camera on a Mobile Robot, Advanced Robotics, (2002).

[24] PASSOLD, F.—STEMMER, M. R.: Feedback Error Learning Neural Network Applied to a Scara Robot, RoMoCo'04, Proceedings of the Fourth International Workshop on Robot Motion and Control, (June 17-20, 2004), Puszczykowo, Poland, 197–202.

[25] BOUTARFA, A.: A New Approach to Beacons Detection for a Mobile Robot Using a Neural Network Model, RoMoCo'04, Proceedings of the Fourth International Workshop on Robot Motion and Control, (June 17-20, 2004), Puszczykowo, Poland, 384–389.

[26] ACHOUR, K.—DJEKOUNE, O.: Incremental Hough Transform: an Improved Algorithm for Digital Device Implementation. Real Time Imaging, Elsevier,, 2004.

[27] CHENG, I.—BOULANGER, P.: Feature Extraction on 3D TexMesh Using Scale-Space Analysis and Perceptual Evaluation, IEEE Transactions on Circuits and Systems for Video Technology, Special Issue (October 2005).

[28] GRADINARIU, M.—DATTA, A.: A Short Introduction to Failure Detectors for Asynchronous Distributed Systems, ACM Sigact News, Distributed Computing Column, **36** No. 1 (November 2005), 53–70.

Received 11 July 2006

**Abdelhalim Boutarfa** was born in Lyon (France) in 1958. He graduated from Constantine University in Engineering Physics. He obtained the Electronic Engineering Degree from the Polytechnical School of Algiers, the DEA Diploma in Signal Processing at the National Institute of Sciences Applied of Lyon, the Magister in Image Processing and PhD in Computer Engineering from University of Algiers. Since 1987 till now he has taught at the Department of Electrical Engineering in Image Processing. In 2005 he was promoted to Associate Professor. His research interests include artificial intelligence and applications, modelling, identification, and computer vision.

**Nour-Eddine Bouguechal** was born in Bizert, Tunisia, on the 18th of November 1953, of Algerian Nationality. He received the degree of Electronics Engineer in 1976 from the National Polytechnical School of Algiers and the Magister (Master) in Nuclear Engineering from the Nuclear Centre of Algiers in 1978. He obtained his PhD degree in Engineering in 1989 from the University of Lancaster, UK. He has been working from 1976 until 1980 in the Nuclear Centre of Algiers in the Reactor Group. From 1981 until now (2005) he has been working as a lecturer and as a full time Professor of Electronics. He has been Director of the Institute of Electronics, Vice-President for Postgraduate Studies and Scientific Research and Dean of the Faculty of Engineering as well as Director of the Advanced Electronics Laboratory of the University of Batna. His main interests are Robotics, Mobile Robotics and FMS and FMS, Microprocessors, Programmable Logic, Signal Processing, Telecommunications and Microelectronics (ASIC Design in collaboration with TU-Berlin). Nour-Eddine Bouguechal is the author of numerous publications for conferences proceedings and journals.

**Hubert Emptoz** is an engineer in Electronics; he obtained the PhD in signal processing. At present he is professor senior and head of the laboratory of vision and pattern recognition at the National Institute of Applied Sciences of Lyon, France. He published several science papers in various journals and gave many lectures in international conferences. His main interests are pattern recognition, signal processing and handwritten word recognition.